THE IMPACT OF SURFACE FINISH AND ORGANIC ADDITIVES ON THE SHEAR BEHAVIOR OF EXTRUDED CERAMIC PASTES

BY

PAUL E. SWARTS JR.

A THESIS
SUBMITTED TO THE FACULTY OF

ALFRED UNIVERSITY

IN PARTIAL FULFILLMENT OF THE REQUIREMENTS
FOR THE DEGREE OF

MASTER OF SCIENCE

IN

MATERIALS SCIENCE AND ENGINEERING

ALFRED, NEW YORK

April, 2015

THE IMPACT OF SURFACE FINISH AND ORGANIC ADDITIVES ON THE SHEAR BEHAVIOR OF EXTRUDED CERAMIC PASTES

BY

PAUL E. SWARTS JR.

B.S. SUNY BROCKPORT 2004

SIGNATURE OF AUTHOR_____

APPROVED BY_____

DR. WILLIAM M. CARTY, ADVISOR

_____

DR. DANIEL E. MCCAULEY, ADVISORY COMMITTEE

_____

DR. MATTHEW M. HALL, ADVISORY COMMITTEE

_____

CHAIR, ORAL THESIS DEFENSE

ACCEPTED BY_____

DOREEN D. EDWARDS, DEAN
KAZUO INAMORI SCHOOL OF ENGINEERING

ACKNOWLEDGMENT

I would like to express my sincere thanks to my advisor Dr. William M. Carty, my supervisor Dr. Daniel McCauley, and all my professors, classmates, co-workers, family, and friends for their guidance and help during the course of this work. Their patience and support were particularly appreciated during the final experiments and throughout the entire writing and review process.

A very special thanks to my wife Catie, for encouraging me to achieve this level of education, and for providing me with support throughout my education. During this time she took on more than her fair share of work. This allowed me to focus on compiling results and writing each evening. Her patience and understanding have been invaluable during this process.

I would also like to thank my employer, Corning Incorporated, for its financial support which allowed me to pursue my graduate education at Alfred University, which includes research for this thesis. Corning also provided me with the means and support by which to conduct the experimentation in this thesis.

TABLE OF CONTENTS

LIST OF TABLES

Page

LIST OF FIGURES

Page

ABSTRACT

The contribution of die-wall friction in ceramic extrusion systems is a variable that has been studied to only a limited degree. The introduction of abrasion-resistant surface coatings, now a common practice in industry, and their associated roughness, is an important area that requires study. To determine the contribution of surface roughness, and the potential to understand that factor in extrusion processes, simple alumina extrusion batches with two levels of a surfactant (a fatty acid), were evaluated.

The goal was to use wall pressure as a function of temperature (°C) and linear extrusion velocity (mm/second) to derive the constants for wall shear behavior constant (β) as well as rate dependent constant (n). Constraints included: four capillary die surface finishes, temperature testing capability ranging from 10°C to 60°C, extrusion noodle velocity up to 50.8 mm per second, and two alumina based extrusion batches designed to elicit a low and high wall pressure response, with which substrate surface finish and capillary wall pressure relationships were developed.

Through minor changes in batch composition, two stable wall pressure regions were achievable without concern of temperature sensitivity. On a high wall pressure batch, varying roughness of the capillary wall surface yields mean pressure differences with little difference in slip behavior. Addition of 0.8% total fatty acid reduced wall pressure to a level where varying roughness of the capillary wall surface yields differences in wall slip behavior. The above modifications were able to produce a range of shear rate behavior constants allowing for the understanding of the interaction of surface finishes when combined with high and low wall pressure extrusion batch.

INTRODUCTION

Extrusion is an important forming process in the ceramic industry for simple and advanced products ranging from bricks to honeycomb ceramic catalysts.[1] To produce cordierite-based ceramic bodies in high volume, the invention of a unique extrusion die was required.[2] With this invention, the premise of plug flow could be applied to establish a constant manufacturing process, however, the rheology of a paste through a die needs to be maintained in a way such that sustainable operation was possible. Plug flow alone could not describe the behavior of the ceramic paste which, as used in this work, refers to highly filled mixtures of particles in a continuous liquid or binder phase.[3] In extrusion, the typical ceramic paste comprises of inorganic particles (of different size ranges), dispersing agents, binders, plasticizers, in a liquid phase, but the knowledge of the impact of surface roughness on die land pressure behavior is limited.[4] Plug flow ignores these surface conditions limiting the ability to accurately predict pressure due to rheological interactions of the batch with the wall.

Models developed by W.H. Herschel and R. Bulkley[5], in conjunction with those developed by John Benbow and John Bridgewater[6], better explain pressure effects of a ceramic paste along the die surface also known as the die land. The six parameter model developed by Benbow and Bridgewater can be used to compare the die land pressure response to a surface thus extracting the key parameters needed to define the interaction of different paste compositions with varying surface roughness.

The objective of this project was to develop a deeper fundamental understanding of batch to wall surface morphology interactions. Using previous rheological work as a guide, a range of hole surface finishes were manufactured. Each surface, representing different levels of large scale waviness (Wa) and fine scale surface roughness (Ra), was extruded upon to separate the overall wall pressure effect of varying organic additives, velocity, and temperature.

In the interest of separating effects of surface finish, surfactant addition, surface finish, and temperature, key assumptions were made. Figure 1 and Figure 2 further illustrate these concepts.

1. The expression of lubricant from the batch compositions chosen serves as a physical interface between the flowing batch and the die surface.
2. The capillary die surface is inert thus drilling/coating method to reach targeted roughness and waviness is not affected by chemical interactions.
3. The particle size distribution of the batch is of an appropriate size as to not become trapped and pack within the micro roughness structure of the coating creating an additional slip behavior outside the capability of testing for this work.

Figure 1. Lubricant serving as an interaction between batch particles and surface finish without chemical interaction.

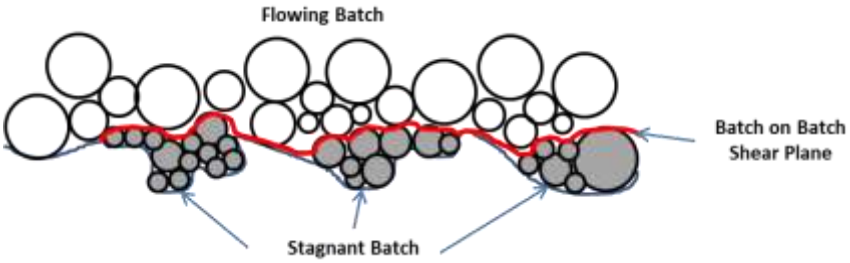

Figure 2. Illustration of particle entrapment on a rough surface.

BACKGROUND

A. Understanding Rheological Behavior

Rheology is a term referring to the study of the deformations, flow characteristics, and viscous behaviors of fluids, suspensions, and forming bodies that occur over the full range of applied shear conditions. It is a broad subject encompassing both Newtonian and non-Newtonian fluids.[5] This area of science is concerned with the response of materials to applied stresses resulting in irreversible viscous flow, reversible elastic deformation, or a combination of the two.[7]

The flow properties of a paste can be defined by its resistance to flow, viscosity, and can be measured by determining the rate of flow through a capillary.[7] The shear stress (τ_s), is the product of the shear strain rate ($\dot{\gamma}$) and material viscosity (η) as shown in Equation 1:

$$\tau_s = \dot{\gamma}\eta \tag{1}$$

If the viscosity (η) of a paste is independent of the shear strain rate, it is an example of Newtonian behavior. However, a number of pastes used in the ceramics industry contain relationships where viscosity is dependent on the shear rate. These behaviors are classified as non-Newtonian and are not limited to one general form.[8] The curves in Figure 3, often referred to as flow curves, are frequently used to describe the rheological behavior of liquids and pastes. Unlike the linear behavior of Newtonian fluids, shear dependent (non-Newtonian) flow is indicated by curves of varying shape, which change behavior with the increase in shear rate. As displayed in Figure 3, shear thinning and thickening behaviors of both Newtonian fluids and viscoplastic (Bingham) materials.[5,9]

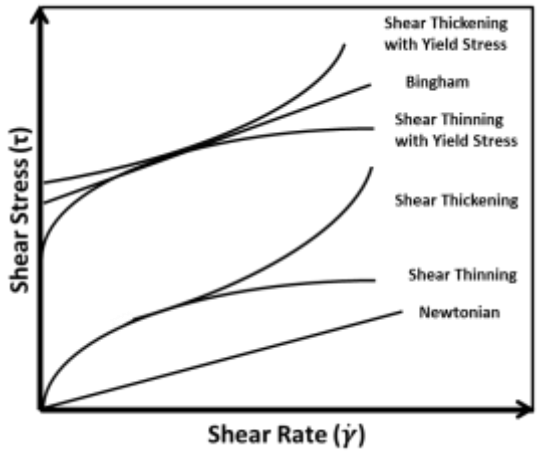

Figure 3. Examples of the six main types of time independent flow behavior. Edited from 9

When focusing on ceramic paste rheology, the typical focus is on non-Newtonian behaviors, in particular, shear thinning, Bingham, and shear thickening (dilatant). To achieve a plastic flow behavior, a yield stress (τ_y) must be exceeded, however the benefit of having a critical yield stress is that a paste is able to hold a shape after forming.[5] A typical qualitative definition would describe yield behavior as a rapid change of a material to a less resistive, or viscous, state. In Figure 3, the yield stress of a non-Newtonian shear thinning material is represented by the y-intercept of the flow curve.[10] As the shear rate increases in pseudoplastic materials, shear-thinning behavior takes place non-linearly. This results in the shear stress curve bending towards the shear rate axis sharply. This demonstrates the shear thinning property of ceramic materials which makes it easier to reach higher shear rates with very little addition of shear stress.[9]

At some point, an increase of shear rate can become great enough to induce a dilatant blockage. Dilatant behavior as a result of particle-particle interactions which change with increasing shear rate is apparent in highly solid loaded paste applications such as pumping, mixing, storing, etc. This is an extreme case of particle collisions causing a sudden increase in viscosity, with an increased probability of a blockage. If severe enough, a cascading blockage occurs within a system and all flow will cease.[5]

B. **Evolution of Rheological Models**

The power law model described in Equation 2 is a commonly used model for rheological systems used to describe time independent rheology such as Newtonian, shear thinning, and shear thickening through the use of the flow behavior index (n).[7,8]

$$\tau_s = K\dot{\gamma}^n \tag{2}$$

The flow behavior index can be determined from experimental data. Plotting and fitting a power law trend line to the shear stress (τ_s) versus the shear rate ($\dot{\gamma}$) is a straight forward procedure to quantify the shear behavior of a of a non-Newtonian paste, as well as make comparisons to other samples.[10] To test the behavior, the n value is simply the exponent of the trend. If n = 1 the suspension is Newtonian, if n < 1 the suspension is shear-thinning, and if n > 1, the flow is shear-thickening or dilatant.[7,8]

Speaking directly to the flow of ceramic pastes, the viscosity can be approximated through the use of the Herschel-Bulkley equation as seen below in Equation 3:[1]

$$\tau_s = \tau_y + K\dot{\gamma}^n \tag{3}$$

In this formula, the shear stress (τ_s) is equal to the sum of the yield stress (τ_y) with the product of the coefficient of rigidity (K) and the shear rate ($\dot{\gamma}$) raised to the flow index (n). When the yield stress (τ_y) = 0, the rheology is classified as non-yield stress. When τ_y is > 0 the rheology is said to be a yield rheology.[5] There are also cases where the coefficient of rigidity (K), Newtonian viscosity constant (μ), and Bingham viscosity (μ_B) can be interchanged with each other to represent different yield dependent rheology. Table V gives an overall summary of the rheological symbols and terms used in this work, which are used in the comparison of time independent rheology equations and their dependence on the flow behavior index (n) as seen in Table I: [5,9]

Table I. Comparison of Time Dependent Rheology[5,9]

	Equation	n	
Yield-Dependent Shear Thickening (Dilatant)	$\tau_s = \tau_y + K\dot{\gamma}^n$	n > 1	(4)
Bingham	$\tau_s = \tau_y + \mu_B\dot{\gamma}^n$	n = 1	(5)
Yield-Dependent Shear Thinning (Pseudoplastic)	$\tau_s = \tau_y + K\dot{\gamma}^n$	n < 1	(6)
Shear Thickening (Dilatant)	$\tau_s = K\dot{\gamma}^n$	n > 1	(7)
Newtonian	$\tau_s = \mu\dot{\gamma}$	n = 1	(8)
Shear Thinning (Pseudoplastic)	$\tau_s = \mu\dot{\gamma}^n$	n < 1	(9)

C. **Extracting Wall Shear Stress from Ram Extrusion Data**

Understanding the flow behavior of highly concentrated solid-liquid pastes is critical in extrusion manufacturing techniques. Benbow, Bridgewater, and Oxley conducted research to refine fundamental rheology models describing the shear stress through a square entry die.[6] Back pressure data for the die entry and land used in these models can be collected through a capillary rheometer, illustrated in Figure 4.

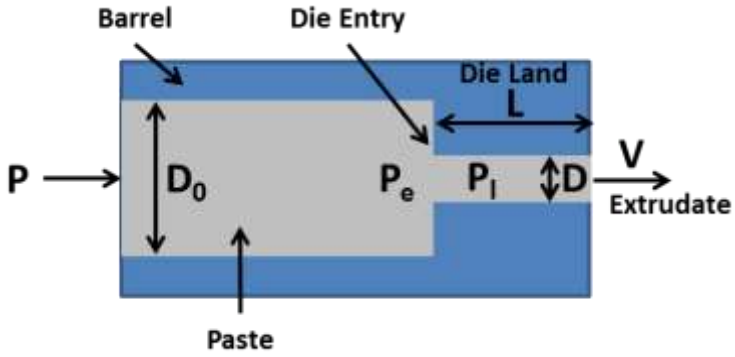

Figure 4. Total extrusion pressure (P), die entry pressure (P_e), and die land pressure (P_l) of paste through square entry die in a capillary rheometer.

Simply stated, the overall pressure drop (P) of the setup in Figure 4 is the sum of the pressure drop at die entry (P_e) and the pressure drop over the die land (P_l).[6] Assuming constant temperature, the generalized description of batch rheology was refined into a six parameter model shown in Equation 10 with the key parameters in red.

$$P = P_e + P_l = 2(\boldsymbol{\sigma} + \boldsymbol{\alpha} V^{\boldsymbol{m}}) ln\left(\frac{D_0}{D}\right) + \left(\frac{4L}{D}\right)[\boldsymbol{\tau_0} + \boldsymbol{\beta} V^{\boldsymbol{n}}] \quad (10)$$

Pressure drop at die entry describes the pressure resulting from the deformation of the batch as it transitions from the barrel to the die. The die land pressure, alternatively referred to in this body of work as wall pressure, is measured through the resulting pressure drop as batch travels along the die surface. Table II describes the terms as they relate to the model above.

Table II. Key Factors in Six Parameter Rheology Model[11-13]

	Symbol	Meaning
General Terms	V	Batch Extrusion Velocity
	D	Die Land Diameter
	D_0	Capillary Barrel Diameter
	L	Die Land (Wall) Length
Entry Pressure Specific Terms	$\boldsymbol{\sigma}$	**Bulk Yield Stress**
	$\boldsymbol{\alpha}$	**Velocity Sensitivity Factor**
	$\boldsymbol{m}$	**Bulk Velocity Exponent**
Land (Wall) Pressure Specific Terms	$\boldsymbol{\tau_0}$	**Initial (Rest) Stress of Paste**
	$\boldsymbol{\beta}$	**Die Land (Wall) Velocity Factor**
	$\boldsymbol{n}$	**Flow Behavior Index**

The final piece necessary in understanding the wall behavior of a batch is the shear stress at the batch/wall interface layer. As material moves, only a thin layer near the wall is subject to shear stress. The pressure drop in the die land (P_l) generates a net force on the paste which is opposed by the wall shear force given by the product of the wall stress (τ_ω) and the wetted perimeter of the die land. Using the experimental wall pressure we get the expression for τ_ω as in Equation 11 for a constant velocity and temperature:[3]

$$\tau_\omega = P_l\left(\frac{D}{4L}\right) \quad (11)$$

Combining back pressure information gathered from experimentation, equation 10, and equation 11 leads to the key expression for this thesis. Assuming the rest shear stress

(τ_0) is negligible and die geometry is constant, Equation 12 is an expression which allows us to experimentally extract wall shear stress (τ_ω), β, and n from wall pressure data:

$$\tau_\omega = P_l\left(\frac{D}{4L}\right) = \left(\frac{4L}{D}\right)[\beta V^n]\left(\frac{D}{4L}\right) = [\beta V^n] \tag{12}$$

Experimentally, these values can be obtained allowing investigation of wall pressure along the land of a die, but this formula will only assess the geometrical impact of capillary geometry on wall pressure interactions. By going one step further, making capillary dies with varying drilling and surface treatment, at the same L/D; the relationship of surface finish on batch/die surface interactions can be evaluated and is the focus of the work described in this thesis.

D. **Adjusting Waviness Through Capillary Hole Manufacturing Techniques**

Forms of roughness in surface finish can be grouped into basic categories, namely roughness, waviness, spacing, and hybrid. These key components, when varied, can create significant shifts in batch/die shear interactions. To create viable options for extrusion experimentation, capillary surfaces must be manufactured to produce distinctly different surface finish characteristics, namely waviness. Waviness is a large wavelength surface texture which forms the base for the superimposition of micro-roughness. Waviness is measured by the arithmetic mean deviation of absolute ordinate values (Z(x)) from a plane fit within a sampling length (L) as seen below in Figure 5 and described in Equation 13.[14]

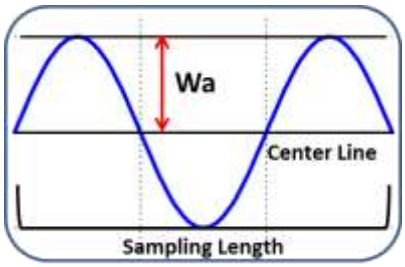

Figure 5. Visual representation of the waviness component of surface finish. Edited from 14

$$W_a = \frac{1}{L}\int_0^L |z(x)|dx \tag{13}$$

Holes created via conventional machining processes, such as turning or milling, rely on a drill bit with varied rotational speeds and feed rates. This creates a consistent surface finish and, in this case, can be fine-tuned to give extremely smooth underlying surfaces. This process, however, does not allow for the tuning of long wavelength roughness (referred to as waviness in this thesis) required to create a varied enough surface finish, thus cannot be the sole manufacturing method for this study.

Electrochemical machining (ECM), is a process commonly used for the machining of small and micro-sized holes into hardened and/or brittle aerospace alloys, medical implants, automobile components, electronics, and casting dies and molds via an electrochemical process on conductive materials. This process can be employed in a way which allows for varying long wave length, also called "wavy" surface finishes prior to coating treatment. With the capability of machining high aspect ratios (Hole Length/Hole Diameter), ECM has an advantage over traditional milling and electrical discharge machining (EDM) drilling methods. That is, ECM has a controlled surface finish, there is no residual stress added to a work piece, low tool wear, no burring or hole distortion, and with the proper rig can support multiple hole drilling.[15,16]

In the ECM process, an electrolytic cell is formed by the tool (cathode) as it is advanced into the work piece (anode) with an electrolyte (weak acid) flowing between them serving as a dielectric gap. Pulsing current across the electrolytic cell agitates the weak acid promoting the reaction. When sufficient voltage is applied, the tool dissolves the work piece in accordance with Faraday's law.[17] Using a weak acid to facilitate the dissolution of material via removal of metal ions enables this technique to achieve very smooth surface finishes with closer tolerances than traditional machining methods when applied to deep holes with high aspect ratios.[15,18]

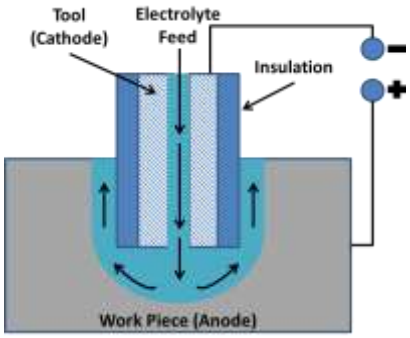

Figure 6. Schematic of the electrochemical machining process. Edited from 15

In the optimal case, the feed rate and the rate of dissolution of the material will be optimized to yield a smooth surface with close tolerance; however, this is not always the desired result. In many fields, including turbine engine manufacturing, high temperatures are required for optimal efficiency; however, the temperatures typically seen in gas turbines would damage turbine blades without some form of cooling hole machined in the blades. In another step towards optimization of the original cooling channel proposed in a patent by W.N. Peters[16], the idea of adding turbulation, or periodic changes in the inner diameter, of the channel was instituted to increase the heat transfer rate as well as add turbulent flow to the cool air being passed through the blades. This same process would add a sufficient level of hole surface finish to the capillary dies being used in this study. Through adjusting the feedrate algorithm for a specific turbulator shape, waviness can be imparted upon the metal hole which can be measured through the waviness (Wa) parameter of surface finish.[14,19]

E. **Adjusting Roughness Through Capillary Wear Resistant Coating Techniques**

While drilling techniques are capable of creating large scale surface finish features such as waviness in a die wall, finer irregularities in surface texture must be created via more subtle means. The resulting surface roughness is measured via a similar method to waviness; however, the measurement technique must allow for the exclusion of waviness components. The method of measuring roughness is described as the arithmetical mean deviation of all peak values from a plane fit along a sampling length of the test part surface. While the variables are the same, this definition varies from waviness in that instead of using a plane fit to the waviness data the plane fit is to the actual surface of the part. This is visually represented in Figure 7 with the arithmetic form in Equation 14.[14]

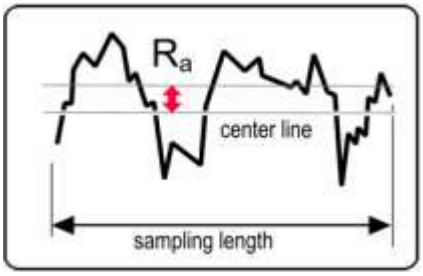

Figure 7. Visual representation of the roughness component of surface finish.[14]

$$R_a = \frac{1}{L}\int_0^L |z(x)|dx \tag{14}$$

Coatings of varying types and morphologies are a way of achieving subtle differences in micro scale surface roughness required for creating desirable surface finish. For over a decade, nitride-based protective coatings, such as TiN, have been an industry standard in the tooling industry due to their excellent wear resistance. Through the use of solid solution hardening, ternary TiCN films were identified as having high hardness, low friction coefficients, and excellent wear properties, hence are widely used in various applications, such as tools and dies, which require long term wear resistance with a relatively low coefficient of friction.[20]

Given the constraints of this project, it was desirable to produce effective surface roughness differences while using the same general process at similar coating thickness. Lin, Moore, Pinkas, Zhong, and Sproul found that the formation of TiCN with the addition of boron as a precursor, can effectively reduce the coefficient of friction (COF), while maintaining good mechanical properties and strength of TiCN coatings.[21] The key driver in the reduction in COF is from a marked difference in crystalline growth, namely, a much finer crystalline structure.[22] TiBCN films can be synthesized by applying the same methods as their TiCN counterparts. Table III and Figure 8 show the result of using a Boron dopant on thin coatings (1μm thick). The grain sizes range from 2.6 to 3.2 nm and surface finish roughness (Ra) in the 14-22 nm range.[20]

Table III. Deposition Parameters and Film Characteristics[20]

Sample	Target current (A)		Film concentration (at.%)					Grain size (nm)	Roughness (Ra, nm)
	Ti	BC	Ti	B	C	N	O		
TiBCN1	40	50	9.3	8.2	55.4	9.3	17.8		15.9
TiBCN2	50	50	18.7	11.8	38.7	14.2	16.6		18.2
TiBCN3	60	50	27.5	8.9	26.7	18.1	18.7	2.6 nm	22.5
TiBCN4	70	50	33.7	5.5	20.6	19.8	20.4	3.1 nm	14.3
TiBCN5	70	40	37.4	3.7	18.7	27.5	12.8	3.2 nm	22.5
TiN6	60	0	45.4			47.4	7.2	6.3 nm	1.2

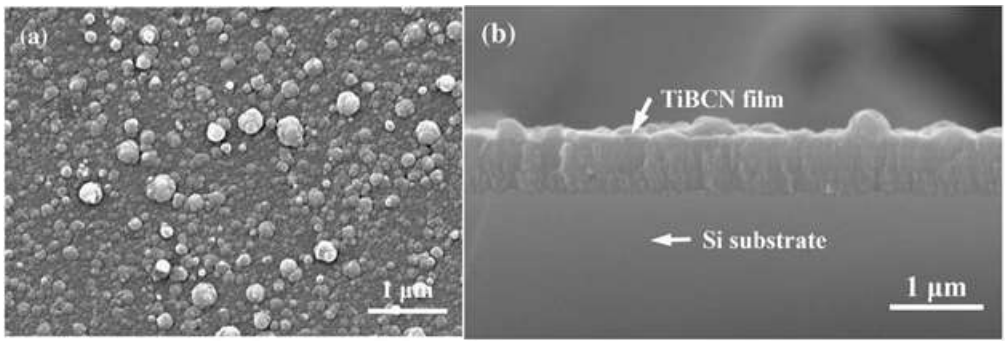

Figure 8. (a) FESEM surface micrographs and (b) cross-sectional FESEM micrograph of TiBCN5 sample.[20]

TiBCN meets the requirement of a reduced COF while still maintaining a process favorable to current manufacturing methods. The morphological differences between TiCN and TiBCN surfaces will promote distinct separation of wall shear effect differences due to batch/capillary die surface finish interactions at the same L/D.

Applying these wear resistant coatings is the final step in establishing the surface finish for the capillaries used in this study. A chemical vapor deposition (CVD) is a common method in the tool and dies industry for coating surfaces due to its continued improvements in capability and equipment design. Coating surfaces via CVD offers opportunity for gas to flow through pores or holes in a surface create monolithic or multi-layer coatings, and film growth with high uniformity. The concept of the CVD coating process is visible in Figure 9.[23]

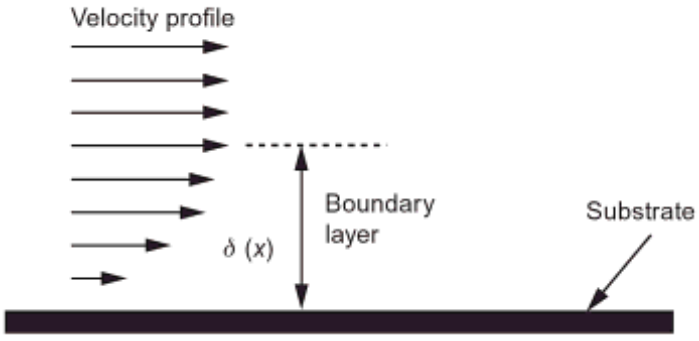

Figure 9. Velocity profile of CVD gas flowing over as substrate surface.[23]

In general, the coating process begins with the preparation of suitable precursors ($TiCl_4$ and CH_3CN) which are mixed together in the correct stoichiometric ratios to form

the desired composition. Additives (such as boron) and process changes (temperature, time, etc.) can be included at this time to tune the properties of the final film to desired thickness, surface finish, and hardness. Once the solution is made, it can then be vaporized. Typically, modern titanium (MT) carbide coatings are vaporized between 700-900°C and transported through the dies via an appropriate carrier gas (H_2 or N_2) where it then nucleates on the hole surface.[22] The desired thickness is ultimately achieved through deposition time at optimal temperature. Over time the resulting TiCN coating is a crystalline structure which offers high wear protection. As fresh precursor gases flowing over the surface is the basis for the chemical reaction to sustain crystalline growth, this process is considered transport-limited. However, the buildup of most coatings is typically slow enough where the boundary layer created by the gas flow profile over the surface is insignificant.[22,23]

EXPERIMENTAL PROCEDURE

A. Experiment Purpose, Scope, and Hypothesis

The purpose of this experiment was to better understand wall pressure response to changes within batch composition and surface finish. A 2^4 factorial designed experiment was constructed to determine how varying four main factors, namely, batch composition, surface waviness, surface roughness, and temperature, would affect the velocity driven wall parameters β and n. Table IV describes the parameters of this experiment.

Table IV. Experimental Factors

Fatty Acid Level	Surface Waviness (Wa)	Surface Roughness (Ra)	Temperature Level
Low	Low	Low	Low
			High
		High	Low
			High
	High	Low	Low
			High
		High	Low
			High
High	Low	Low	Low
			High
		High	Low
			High
	High	Low	Low
			High
		High	Low
			High

The desired outcome was to determine the impact of surface finish and addition of a polar surfactant (fatty acid) on wall pressure behavior. The hypothesized wall pressure reactions were:

1. Starving the system of polar surfactant results in direct interaction between the batch composition and the capillary wall. This was reflected in a higher wall pressure and β value which is undesirable to a high velocity extrusion processes.
2. The n value (wall slip) will increase with the amount of polar surfactant, resulting in a lower velocity dependence (β). While a high n value is desirable, doing this through the addition of fatty acid surfactant alone is not cost effective.
3. Varying the surface texture to produce low β at consistent n values, which is highly desired.

The desired extrusion batch needed to be a base composition at a single batch stiffness value and coarse to fine alumina ratio which, when tested over two levels of fatty acid lubricant, creates high wall pressure and low wall pressure conditions with enough of a difference to generate confidence that the results were outside the variability of the test. While using one batch with both high and low wall pressure regions was possible, the temperature dependent transition region between the two was not consistent thus unpredictable. To prevent interactions within the tested temperature range, batch compositions were chosen through a process of elimination within a 2^3 factorial designed experiment space shown in Figure 10. The dry batch components of the composition summed to 100% by weight with water and fatty acid as super addition to the total dry batch weight.

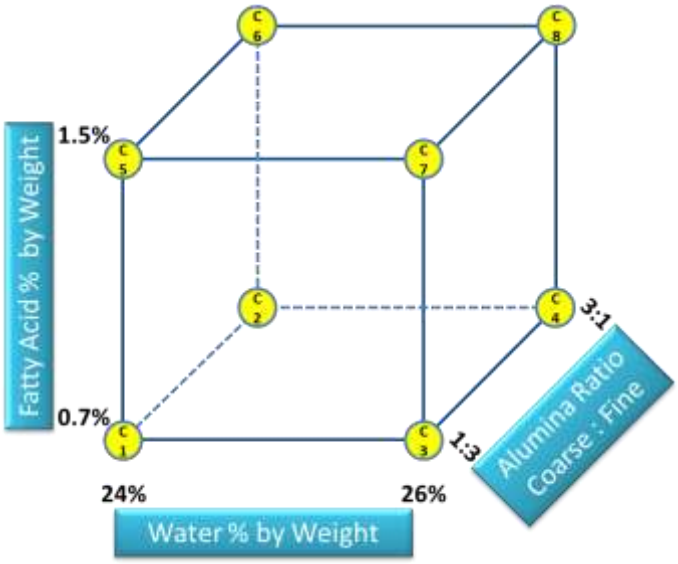

Figure 10. Batch composition operating space includes two levels of fatty acid, water, and coarse to fine alumina ratio.

B. **Tests Used in Experimentation Procedure**

For rheology feedback, a model Rosand RH7 capillary rheomoeter manufactured by Malvern Instruments headquartered in Malvern, UK was employed in experimentation. This piece of equipment was chosen due to its wide use in science/manufacturing facilities, robust design, and flexibility in measuring various materials including polymers and

ceramics. The documented temperature range of this piece of machinery is 5°C to 200°C using a pressure transducer rated to 70 MPa with a data collection frequency of 1 data point per second for the temperature sweep test, and 100 data points per minute for the velocity sweep test, both of which are described below.

The first of the two tests on this equipment, a temperature sweep, is intended to look for temperature dependent wall pressure behavior. The test was run at low velocity over a set temperature range and rate to determine the temperature sensitivity of the batch. The drawing in Figure 11 demonstrates the multiple regions that can exist for one composition, namely high wall pressure at low temperature (Region 1), wall pressure transition (Region 2) , low wall pressure at high temperature (Region 3), and high temperature batch stiffening (Region4). In this test, the temperature range was 10°C to 60°C at a rate of 1°C per minute at an extrusion velocity of 12.7 $mm \cdot s^{-1}$.

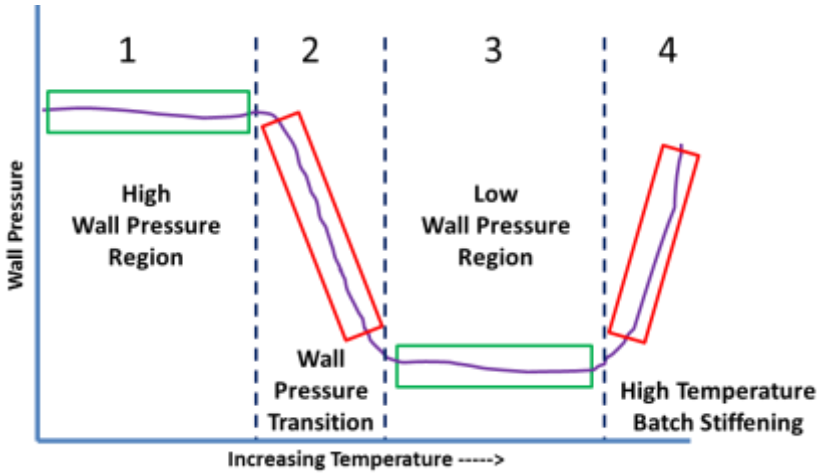

Figure 11. Schematic of temperature sweep study data.

The velocity dependent wall pressure behavior at a temperature where wall pressure behavior is consistent can be determined when piston/noodle speed is stepped down from a relatively high velocity to low velocity. The resulting data can be analyzed to determine if the resulting pressure is a direct response to shear rate or if lubricating wall slip is involved. The standard test parameters for the velocity sweep are described below:

1. The standard velocity sweep test ramps through a range of extrusion speeds determined by the user in order from highest speed to lowest to determine the point at which extrusion slip first occurs.

2. The time duration at each stage uses a pre-programmed window of 15 to 67 seconds. The software determines when stability has been reached leading to variable test time.
3. Raw pressure data for P_{total}, P_{land}, and P_{entry} are output from this test.

Using compositions with an unstable pressure drop, the time allotted for stability is too short. The resulting data for stages with this behavior would be erroneous and require filtering or complete removal from the data set. Figure 12 illustrates the effect of the lack of stability on the back pressure output of the test.

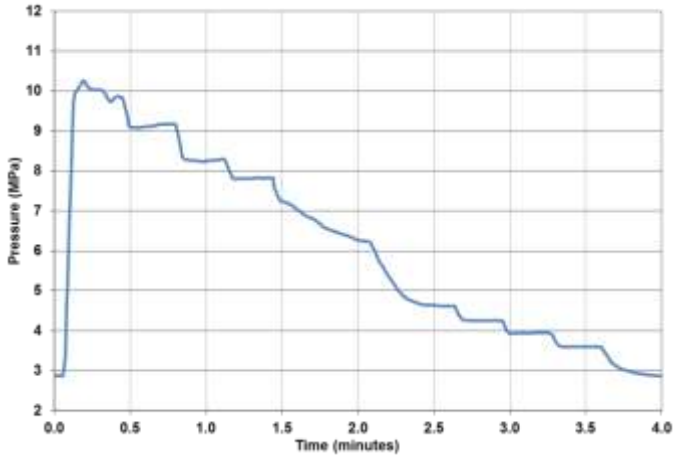

Figure 12. Example demonstrating insufficient stage incubation time during unstable pressure drop between 1.5 and 2.5 minutes.

The stage duration time of the velocity sweep program can be modified to include sufficient time for stabilization. In order to allow for sufficient stabilization time and maximize the data collection time of the velocity sweep test, the stage length was extended to two minutes per stage. Figure 13 demonstrates the change in stage duration.

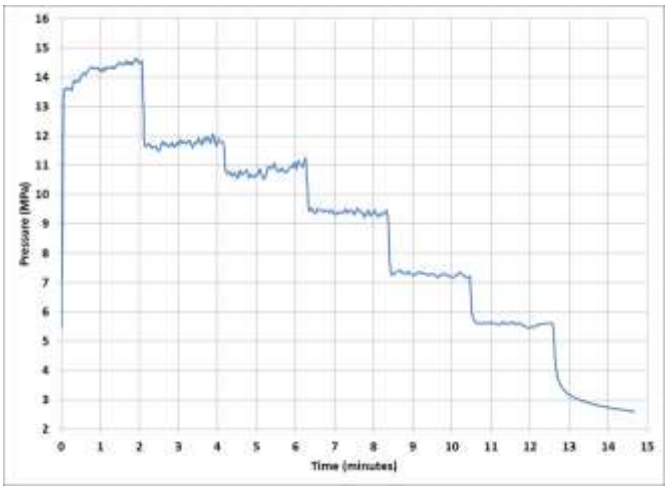

Figure 13. Example demonstrating sufficient stage incubation time.

Analysis of the velocity sweep test yields coefficients which characterizes the effects of surface finish, velocity, and composition on wall behavior. Through testing procedures entry pressure can be separated from total die back pressure to yield wall pressure: ($P_{land} = P_{total} - P_{entry}$). Using the raw wall pressure (at constant temperature) as the input, Equation 11 was used to determine the wall shear (τ_ω) for a given velocity. The plotted wall shear result with respect to extrusion velocity is demonstrated in Figure 14.[3,11]

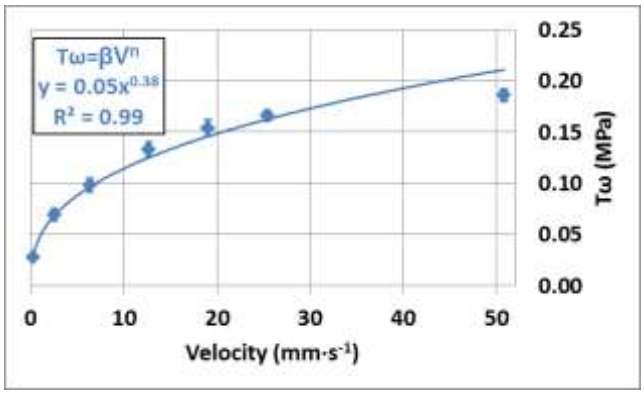

Figure 14. Relationship between calculated wall shear (from wall pressure data) and extrusion velocity.

The power law trend of the resulting plot reveals the terms β as the first term in the trend, and the shear thinning factor 'n' as the exponent of velocity. The factor n is the dependence of the bulk paste yield stress on velocity, and β is the velocity factor of wall shear stress; ($MPa \cdot s \cdot mm^{-1}$). This also enables direct comparison of multiple data sets by

simplifying the overall appearance of the data. Figure 15 demonstrates the log10 transformation of wall shear data and extrusion velocity.

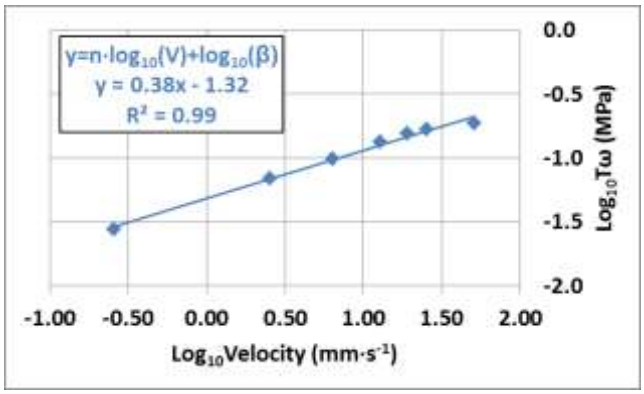

Figure 15. Log_{10} transformation of wall shear stress plotted against log of extrusion velocity reveals the accuracy of the trend fit for predicting β and n.

C. **Capillary Die Preparation**

It was hypothesized that there is some combination of manufactured surfaces that can be experimentally determined to affect pressure evolution. Using a combination of the drilling and coating techniques, two scales of roughness (Ra) and waviness (Wa), as described previously, were used to create capillaries with four total levels of surface finish.

Metal capillary die blanks comprised of stainless steel were drilled using electro-chemical machining (ECM) and traditional milling processes, in this case gun drilling. Using the two drilling methods, a statistically significant difference in hole waviness was created using a 95% confidence interval. The surface waviness result of ECM drilled holes was 0.76 +/- 0.16 μm compared to traditionally milled holes at 0.49 +/- 0.08 μm.

When coating a capillary, the TiCN grain length is used to affect the micro-roughness of the land area. Since both grain length as well as coating thickness grow with respect to time and temperature, an experiment for estimating the optimal roughness was used to determine the micro-roughness at a given thicknesses of TiCN. The result was a relationship which could be used to achieve sufficient micro-roughness to elicit a wall pressure response. Figure 16 and Figure 17 are a coating study representing the correlation of crystalline growth (length) as a function of coating thickness.

	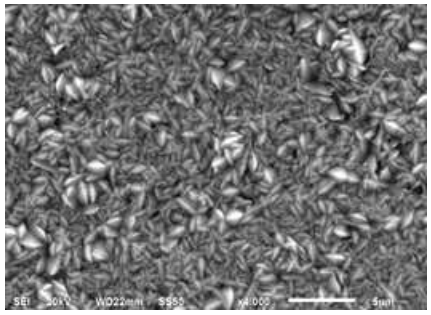	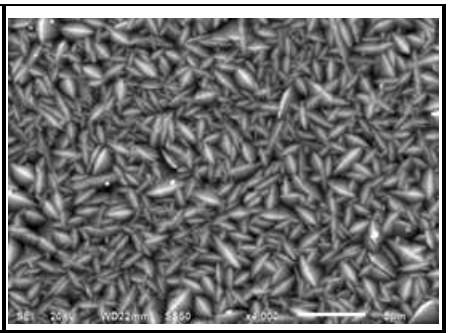
Coating Thickness (microns)	**4.2**	**7.2**
Mean Crystal Length (microns)	**1.4**	**1.8**
	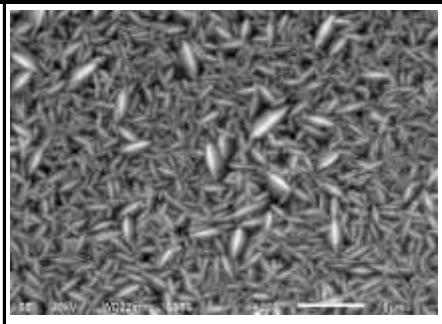	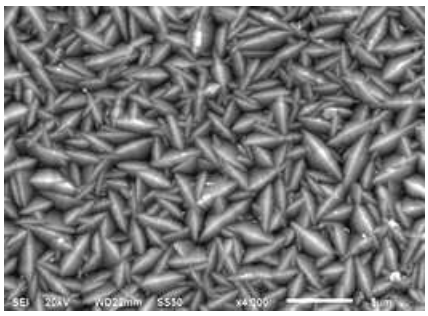
Coating Thickness (microns)	**10.0**	**18.1**
Mean Crystal Length (microns)	**2.0**	**2.9**
	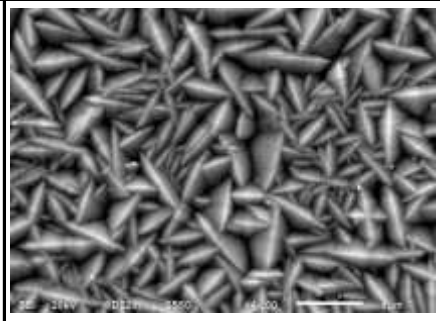	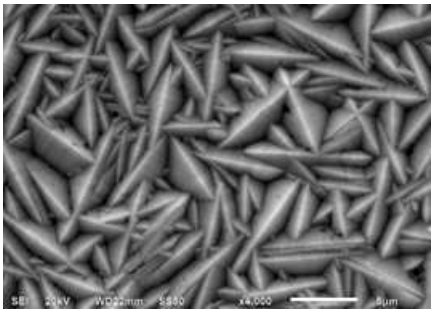
Coating Thickness (microns)	**24.4**	**39.5**
Mean Crystal Length (microns)	**3.6**	**4.7**

Figure 16. Examples of TiCN grain length evolution via JEOL 6610LV SEM.

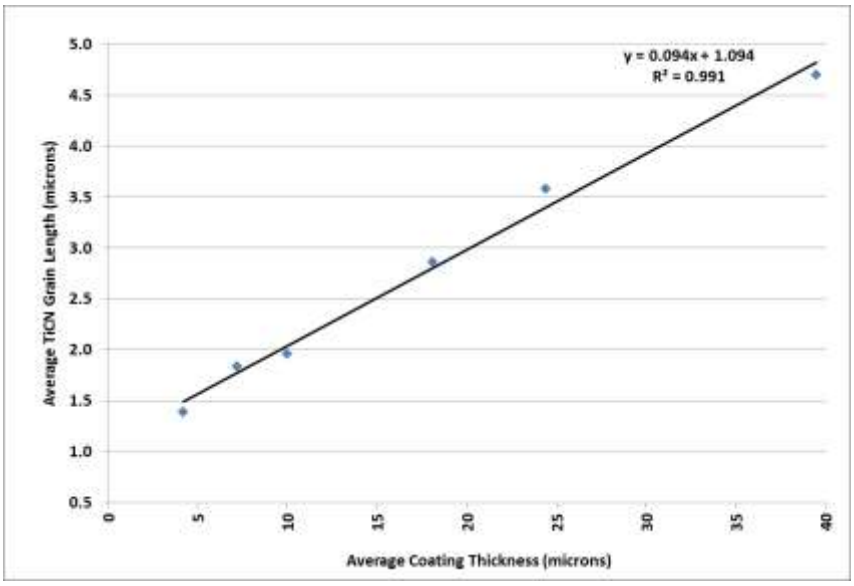

Figure 17. TiCN grain length vs. coating thickness correlation.

Based upon the images and grain lengths in Figure 16 and the correlation Figure 17, the range of coating thickness to create a micro-roughness response while not over coating the capillary die holes used for this experiment was between 10 and 18 microns.

The drilled metal substrates were cleaned using ultrasonic bath of DI water, mild solvents, and then a final rinse was performed using pressurized water prior to coating. The dies were coated with TiCN and TiBCN using chemical vapor deposition (CVD) within a commercial model BPX-pro 750 S CVD reactor manufactured by Ionbond of Olten, Switzerland to create differences in the micro roughness levels of surface finish.

Fifty optical surface profilometer measurements were taken from each capillary via a Zygo New View 6300 manufactured by Zygo Corporation headquartered in Middlefield CT. Given the fine micro scale roughness of the coating, a 2000x magnification setting was used on the exposed surface to capture both the waviness and roughness and confirm the objective of creating varying surface finishes was achieved. The sampling area of each measurement at this magnification was 53μm by 71μm. Figure 18 illustrates the surface finish obtained through the two coating methods.

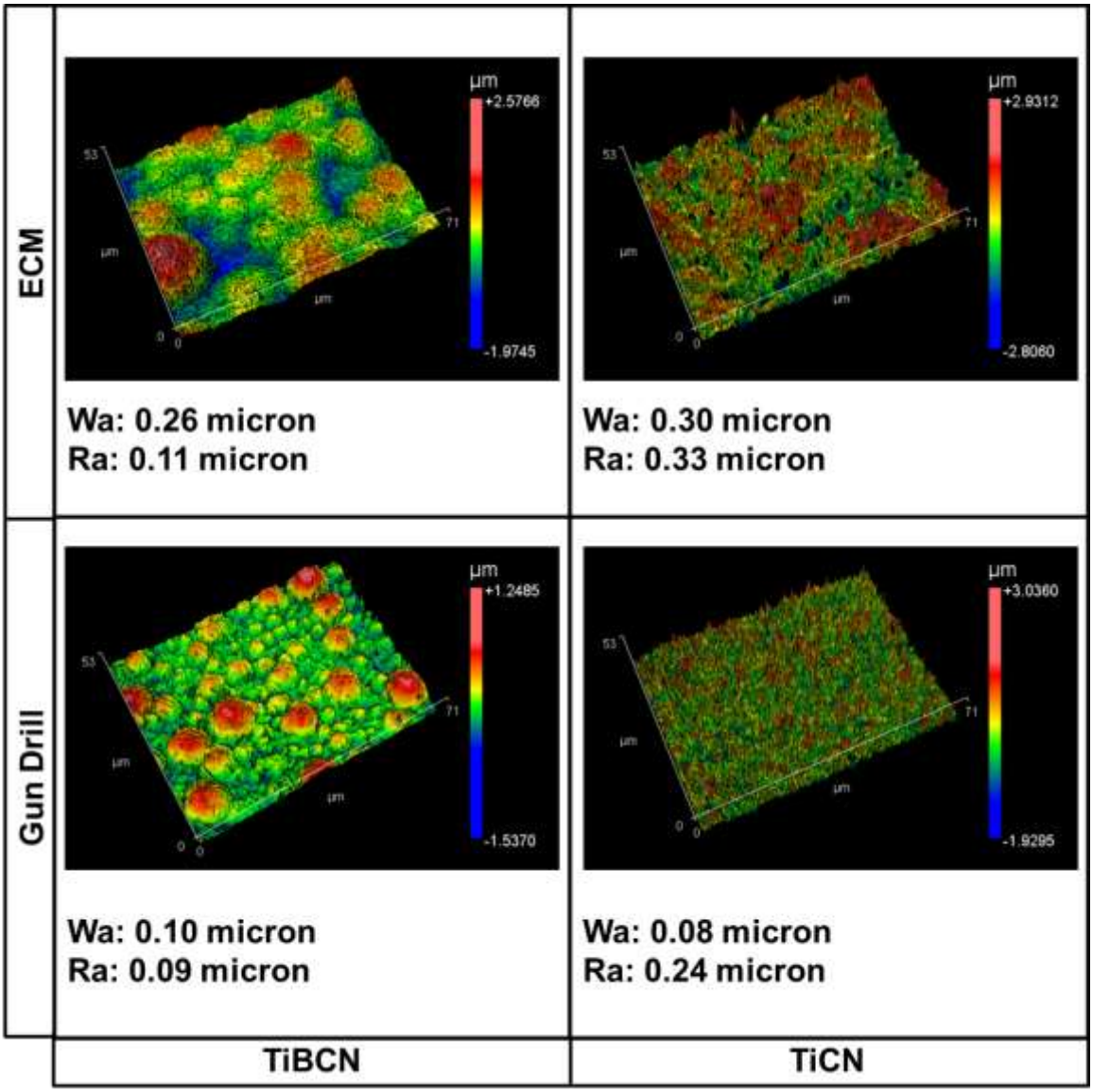

Figure 18. Post-coating optical surface profilometer results.

The final machining of the drilled and coated blanks into cylinders with a nominal diameter of 0.46" (11.684 mm) and nominal length to diameter ratio (L/D) of 28.5 were obtained through a combination of wire electrical discharge machining (wEDM), to form cylinder-shaped substrates, and counter-bored holes to achieve the 28.5 L/D on each die.

D. **Test Procedure**

Cellular extrudate was formed and directly funneled into a cone fixture with a 13mm exit hole diameter which will create a rod form for all samples in this experiment.

This setup for direct extrusion to guide batch flow instead of relying on using multiple steps, torque rheometer mixing, and load frame forming methods was simpler and resulted in more consistent rod to rod rheology.

The key requirements of the two batches chosen for investigation were to have stable pressure at two temperatures. This meant that the high and a low wall pressure behavior must be within Region 1 boundaries (high wall pressure) and Region 3 boundaries (low wall pressure) from Figure 11, and the upper temperature limitations of the batch must be high enough as to prevent the occurrence of batch stiffening as seen in Region 4 of Figure 11 during testing.

The two batch compositions used in this process were determined from the exploration of the batch composition space described in Figure 10. This testing was accomplished through use of an OEM Malvern Tungsten Carbide capillary die and a sustained feed rate over the course of ten minutes. The entry pressures (0.5 mm die length) from this test established the relative stiffness of the batch entering the die to determine water level, while the wall pressure behavior would determine the impact of varying fatty acid level on a particular composition.

The final set of tests were the first time the experimental die surfaces would be used in this experiment so, to test the impact of the manufactured capillary surface on batch rheology, low velocity temperature sweep tests were first run on each capillary type to validate wall pressure differences surface to surface. At a stable temperature determined from the previous test, velocity sweep tests will be run to extract β and n values for comparison between the surface finishes and batch compositions. Die run order was randomized and dies were cleaned with solvent, pressurized warm water, and dried between each run to prevent residual fatty acid from affecting wall pressure response of tests run on the same capillary die.

RESULTS AND DISCUSSION

A. Selection of Ceramic Paste Extrusion Material

A preliminary study was conducted at two water levels to gauge the effect of alumina particle size ratio and water content on the difference between entry pressure and wall pressure. Each composition was run for ten minutes at a constant velocity of 50.8 $mm \cdot s^{-1}$ through tungsten carbide capillaries supplied by the original equipment manufacturer (OEM). Of the complete set, the first two minutes of data were removed as stabilization time. The balance of the data was assumed stable and comprised of 480 data points for each combination tested. Medians and standard deviations were calculated and plotted to compare sample distributions.

As illustrated in Figure 10, an alumina paste was required that produced a strong pressure difference to test for the appropriate wall pressure response when combining with various die capillary surfaces. All of the test cases in Figure 19 show a shift in wall pressure with additional surfactant regardless of alumina ratio, however the largest change in median wall pressure was between condition 1 and condition 5, both of which contained a 1:3 coarse to fine alumina ratio at low water percent. The ratio of solid to liquid fatty acid was held constant at ~1:2 through the experiment. The addition of 0.8% excess fatty acid, comprising of 0.27% increase in stearic acid and 0.53% increase in liquid oil, resulted in a 4:1 wall pressure reduction of 2.2 MPa. All other cases maintained consistent mean pressure shifts when transitioning between low and high fatty acid levels.

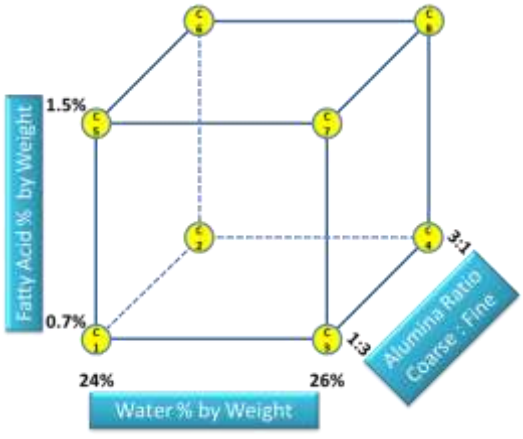

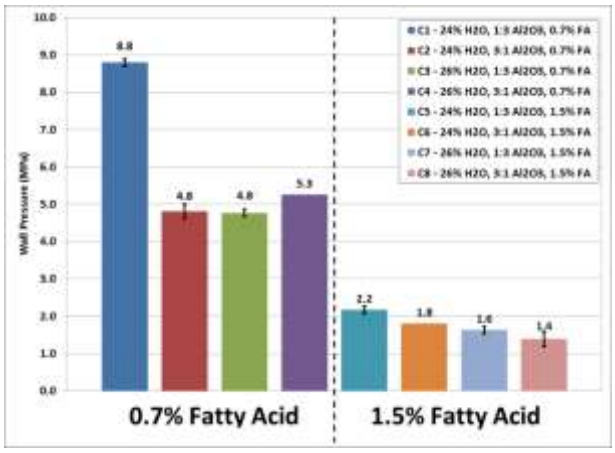

Figure 19. Wall pressure reduction through an increase in fatty acid with respect to water and changes in coarse to fine alumina ratio.

Establishing equivalent stiffness was another requirement prior to using the experimental die surfaces to assess wall pressure behavior. The corresponding die entry pressure difference between condition 1 and condition 5 in Figure 19 was examined to gauge the shear force needed to deform the batch traveling from the barrel of the capillary rheometer into the square entry of the feed hole at two fatty acid levels. The results indicate a 1 MPa difference in entry pressure exists due to fatty acid contribution.

From prior work, entry pressure within a +/- 0.5 MPa range were considered the same thus, to create an equivalent entry pressure response the water level was adjusted to compensate for the difference in entry pressure due to fatty acid levels. Additional testing conducted at both fatty acid compositions verified the water content change needed to reach equivalent entry pressure. The 0.7% fatty acid composition was increased from 24% to 25% water while the 1.5% fatty acid composition was decreased from 24% to 22.7% water. At 22.7% water, the entry pressure delta was reduced from 1 MPa to 0.14 MPa while maintaining a wall pressure difference of 3.6 MPa.

Through this testing, exploration of the space resulted in a single composition which could be used at two fatty acid levels that would elicit a significant wall pressure response while maintaining the same stiffness. By shifting the ratio of coarse to fine alumina particles as well as balancing water content to match entry pressure, a wall pressure reduction of nearly a 3:1 ratio was achieved which would offer ample wall pressure difference at equivalent stiffness.

The hypothesis being tested was that the wall pressure response could be altered by varying surface finishes of a capillary dies. If true, the surface finishes created on the capillary dies used will alter the gap between the high and low wall pressure compositions. Additionally, the strong wall pressure response between high and low fatty acid compositions would be sufficient to assure statistical significance of the final data.

B. **Temperature Dependence of Batch Composition**

Similar to how wall and entry pressure was measured using constant rate versus time to determine the differences in wall and entry pressure of a die, constant rate versus

temperature can be run to determine the temperature dependence of the batch. In this case, the temperature sweep test was run to determine the maximum operating temperature, shown as Region 4 in Figure 11. Conducting measurements above this temperature would lead to stiffening (or a substantial increase in flow resistance/viscosity) and prevent plug flow. For this test the final composition was used in conjunction with the same tungsten carbide dies from the previous section.

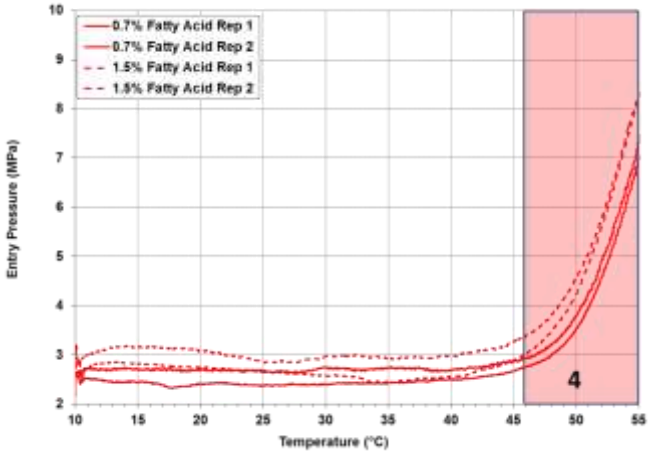

Figure 20. Determining maximum operating temperature limit through capillary entry pressure.

The temperature at which the die entry pressure exceeds the mean pressure between 25°C and 35°C by 15% is considered the point at which critical stiffening has occurred. For the cases tested in Figure 20, the range of these cases fell between 46°C and 47.5°C, so the maximum testing temperature was fixed at 40°C.

C. **Effect of Waviness and Roughness on Temperature Driven Pressure Behavior**

Temperature sweep tests were run on each surface at the two fatty acid levels in order to determine if a difference in wall pressure behavior as a function of temperature and surface finish exists. Each test was run at 12.7 mm per second (extrudate velocity) on a hole approximately 1.5 mm in diameter until batch was exhausted or the test ended due to temperature onset stiffening of the batch. Negative slopes showed that a degree of pressure reduction due to batch warming on all compositions with the roughest surfaces showing the most significant pressure drop. One deviation in the pattern of the slopes was observed with the high waviness (Wa) and high roughness (Ra) surface texture on

compositions with low fatty acid lubricant. Given the consistency of the other runs, this run is being considered as atypical when compared to the trend seen at the higher fatty acid level on the same surface.

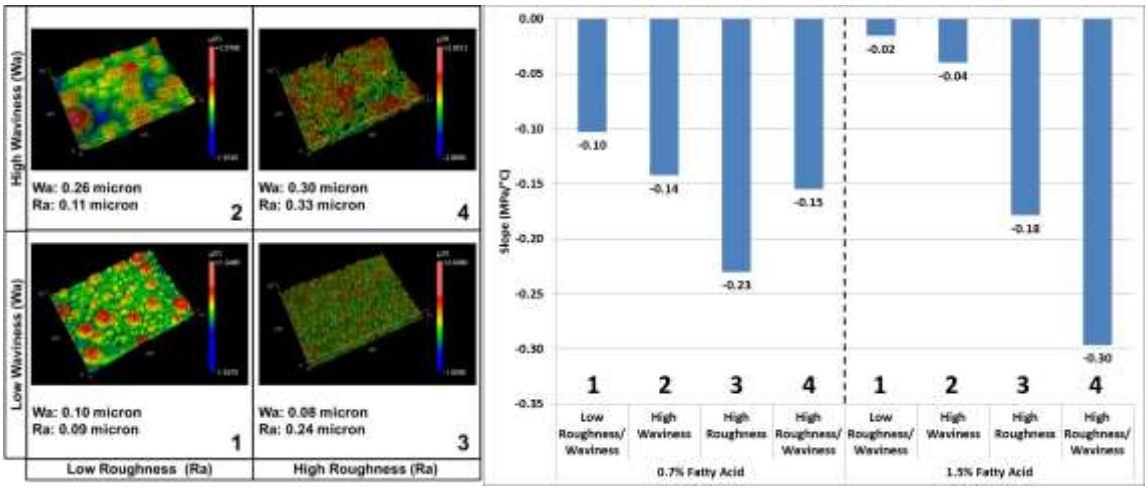

Figure 21. Pressure rate of change (MPa/°C) with respect to temperature stratified by surface finish.

The rate of wall pressure drop with respect to temperature stratifies according to the overall waviness and roughness of each surface. Holes with low overall waviness, combined with a low roughness coating yielded the lowest overall wall pressure and slope with regard to temperature. Increasing waviness and roughness results in higher wall pressure drop with respect to temperature indicating significant surface finish dependent shear behavior.

Based on summarization of the pressure data, it was determined that 10°C and 40°C would be satisfactory temperatures for velocity sweep tests without concern of temperature driven stiffening of the batch or unstable pressure regions.

D. **Effect of Waviness and Roughness on Velocity Driven Wall Pressure Behavior**

It was hypothesized that the wall pressure behavior coefficients, β and n, can be altered using hole surface finish, namely waviness (Wa) and roughness (Ra). In order to understand the effects of these combinations, first it was necessary to gauge the response of each component separately. To measure the impact of waviness, the two drilled surfaces were compared at the smoothest coating level, and to gauge roughness contribution the two coating surfaces were compared on the lowest waviness surface. To extract the coefficients

β and n, the pressure was measured at the stable portion of each stage of the velocity sweep test was converted to wall shear stress (τ_ω), and then plotted against velocity. Through the power law relationship, the wall shear behavior of the composition could be assessed for each wall surface texture.

Low waviness drilled surfaces did not have a significant temperature driven effect at 0.7% fatty acid, however, a significant difference was demonstrated when increasing the fatty acid percent to 1.5%. High waviness surfaces showed both temperature and fatty acid level driven impacts. As seen in Figure 22, the increase of fatty acid lubricant resulted in higher n-values; significantly lowering wall pressure. This supports the observation of high temperature driven pressure drop in Figure 21.

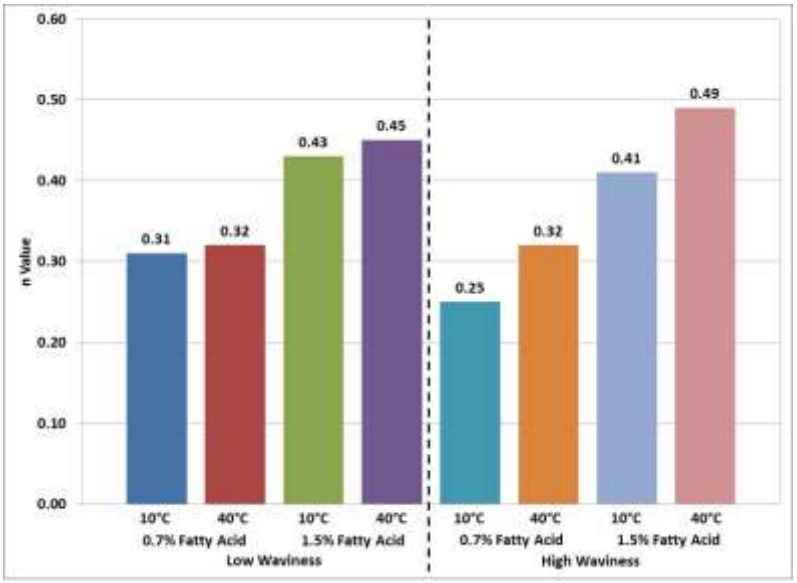

Figure 22. Waviness (Wa) effect on n-value at low and high temperature and fatty acid percent.

There was a discernible difference between the β values of low and high waviness surfaces. At the same temperature and fatty acid level, low waviness surfaces had lower β values when compared to high waviness counterparts. A temperature driven effect within and between fatty acid levels was also present on both surfaces indicating temperature and surface finish could be used to alter wall shear thus sustain higher extrusion velocity without increasing fatty acid level as demonstrated in Figure 23.

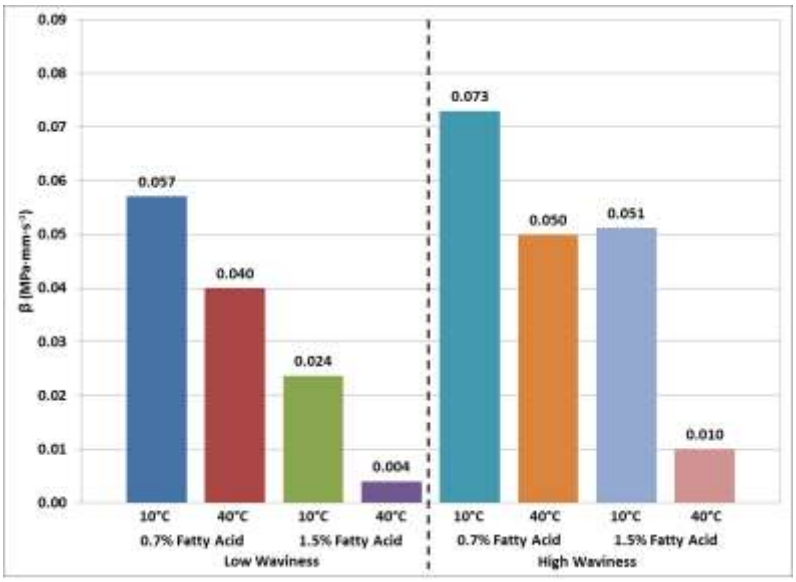

Figure 23. Waviness (Wa) effect on β at low and high temperature and fatty acid percent.

Compared to the smooth surface baseline, frictional forces created by the rough coating resulted in lower n-values at low temperature at both fatty acid levels. Increasing fatty acid alone at 10°C failed to promote improved wall slip behavior at the capillary wall. At higher temperatures, a significant impact was demonstrated on high roughness surfaces at both fatty acid levels resulting in nearly a 2:1 increase in n-value which is favorable to extrusion wall pressure. Through $\log_{10}$ transformation of the data, the increase in n-value was revealed to be due to non-power law pressure drop. This behavior was revealed through the non-linear drop in $\log_{10}$ of wall shear stress with respect to $\log_{10}$ velocity as shown in Figure 25 resulting in a 5% decrease in R^2.

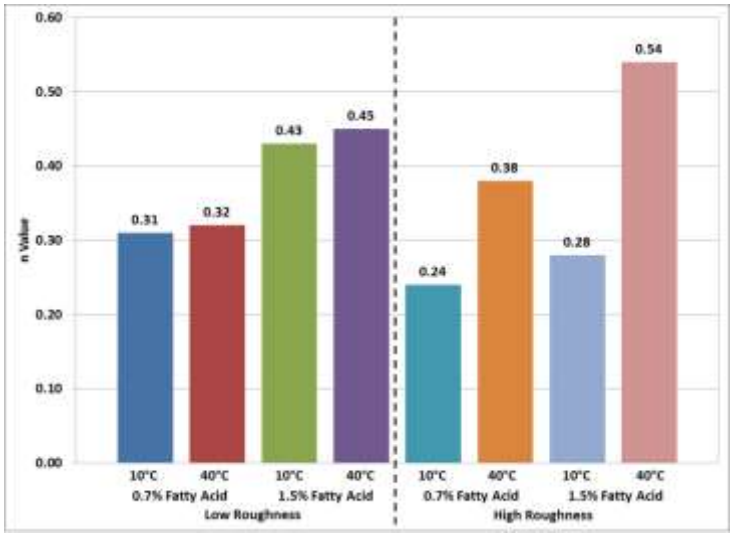

Figure 24. Roughness (Ra) effect on n-value at low and high temperature and fatty acid percent.

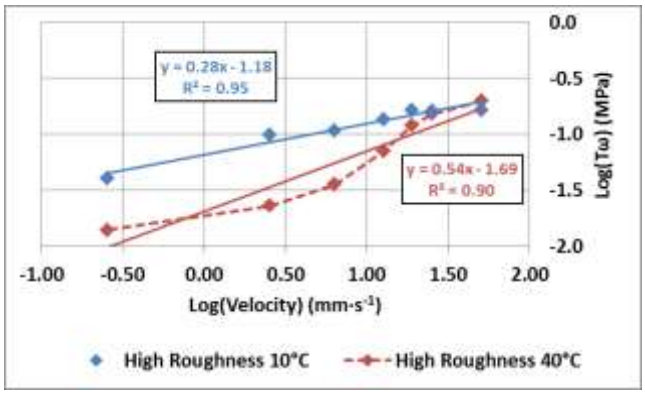

Figure 25. Example of temperature dependence of roughness induced wall shear on behavior.

The wall velocity coefficient β exhibits significant shifts due to Ra both within and between temperature conditions. At low temperatures, the shift from a rough coating surface to a smooth surface demonstrates a benefit, the reduction of β, at both low and high fatty acid amounts, indicating the effect of β is tied closely to surface roughness. When tested at 40°C, the benefit due to the reduction of frictional force is combined with the benefit of lubricant migration to the capillary wall. Examining the differences between low and high fatty acid, rough surfaces benefit the most from this behavior, however, β is much lower using smooth coatings with added fatty acid.

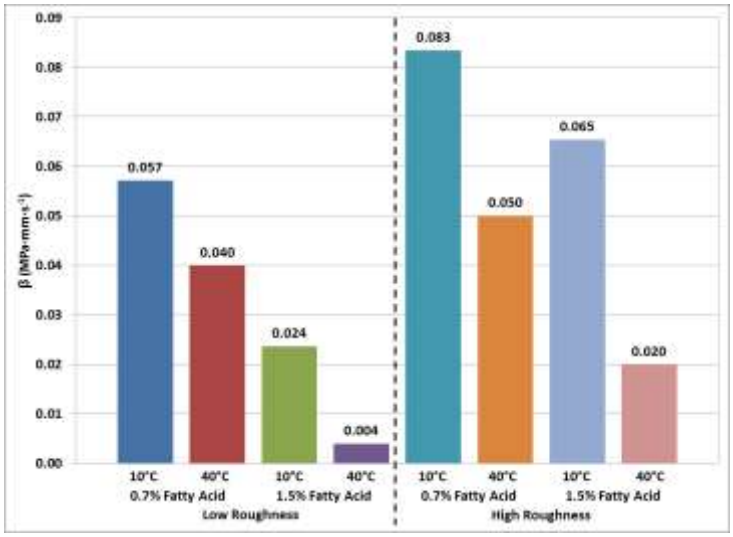

Figure 26. Roughness (Ra) effect on β at low and high temperature and fatty acid percent.

Individually varying waviness and roughness independently of one another gave insight to the contribution of each component. One more step involved combining surface textures to gauge the difference in wall shear behavior between the smoothest and roughest possible surfaces. In Figure 27, the smooth surface behaved as expected at both 10°C and 40°C. Combining the surface finish effects of both a high waviness and high roughness produces extremely high wall velocity sensitivity in the form of a β value over 0.1 MPa·mm·s^{-1}, and low n values at all but the high temperature high fatty acid condition indicating very little lubricant migration is aiding wall pressure. Only at 1.5% fatty acid lubricant and 40°C was this surface able to achieve smooth surface like β and n values. This surface texture combination would not be desirable in high velocity extrusion processes requiring cost effective use of materials.

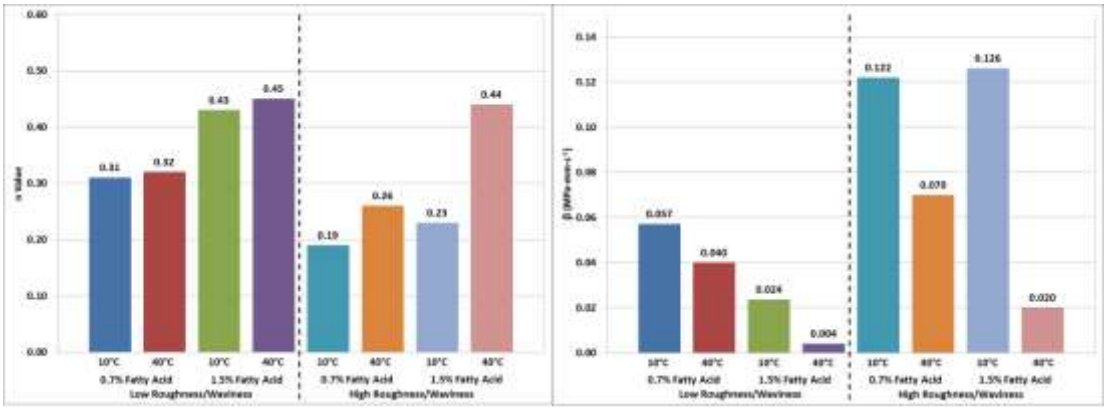

Figure 27. Combined Roughness (Ra) and Waviness (Wa) effect on n and β at low and high temperature and fatty acid percent.

The die land velocity factor β is affected by surface waviness and roughness, fatty acid level, and temperature. Combinations run in this experiment display distinct behaviors. At low temperatures a shift in fatty acid only served to lower the mean β value. When tests were run at 40°C, however, a continuous trend across both fatty acid levels is observed with respect to overall surface texture. This set of tests indicated that not only surface finish could be used as a means to lower velocity dependent wall shear behavior but fatty acid could then be used to fine tune the interaction at distinct

temperatures to presumably enabling expression of lubricant to the capillary wall thus lowering the wall pressure.

The effect of surface finish, fatty acid level, and temperature on the shear thinning index, n, is similar in behavior to β. At low temperatures, fatty acid level did not affect the shear thinning nature of the batch on any of the capillary surfaces tested. At 40°C, however, significant shifts could be seen in n-value grouped by coating roughness. Wall slip effects drove the n-values for rough coatings to the level of smooth coatings, the overall robustness of smooth coated surfaces to temperature variation makes the addition of fatty acid more predictable.

Hole manufacturing technique contributed to both wall pressure coefficients (β and n). Using fatty acid as a method to fine tune shear thinning behavior, the application of both surface finish and fatty acid content produced distinct wall pressure responses and allowed for lubrication content adjustment to achieve optimal operation space for different applications dependent on wall shear effects.

In addition to the combination of surface finish and fatty acid percent, a strong correlation with the temperature has been identified. This is hypothesized to be due to lack of lubricant expression at low temperatures. For example, at 10°C all four surface combinations at both fatty acid percent gave high β and relatively low n-value response compared to the response of the same capillary at higher temperature. At 40°C, all surfaces demonstrated different wall surface behavior at high and low fatty acid percent.

SUMMARY AND CONCLUSIONS

It has been demonstrated that the relative difference in die land velocity factor (β) is directly dependent on the micro roughness of a die, while the shear thinning exponent (n) is dependent on the amount of lubricant (fatty acid) within the batch composition. Using techniques from this body of work, the effects of these components can be taken into account when developing a process to achieve desired wall shear and resulting pressure in the extrusion environment. The effect of surface waviness on extrusion behavior, while present, is not a parameter that creates fundamentally different wall shear stress behavior, nor one that can be changed at as fine a scale as surface roughness. The data analyzed in this work leads to the conclusion that the best methodology to elicit change in extrusion behavior is to focus on combinations of surface roughness and lubrication.

Modifications to commercial batch compositions were successful in creating high and low wall pressure levels to test upon four waviness/roughness surface combinations. While wall shear behavior could be altered significantly using varying surface finishes, fatty acid percent had a significant impact on creating wall "slip" behavior and thus adding another level of control to the wall shear behavior of a batch. Identifying distinctions between extrusion die wall surfaces were possible through the analysis of raw pressure behavior, β-values, and n values.

This translates to the following conditions for optimal extrusion wall pressure behavior:

1. Low micro-roughness surface texture via TiBCN coating type.
2. Low waviness surface texture via gun drilled hole type.
3. Temperature controlled extrusion process to maintain warm batch temperatures either through direct warming of the batch or die.
4. Using small variations in fatty acid surfactant to fine tune the wall pressure result.

RECOMENDATIONS AND FUTURE WORK

Of the capillary dies tested, surfaces with a low roughness coating exhibited the most stable and predictable behavior across multiple lubricant conditions when run at multiple temperatures. It is recommended in future work to test over a wider range of coating surface roughness to assess hole roughness effects on wall shear components. For testing the differences in wall shear behavior due to coating roughness, it is recommended to use low waviness hole surfaces as they were the most stable and reliable in this body of work. The combination of surface with high waviness and high roughness cannot be recommended for process where low temperatures and low levels of lubricant are required.

Overall, the effect of surfaces with varied roughness gave stable results with well-illustrated wall pressure effect, however, this study only covered two lubricant levels and two roughness levels. It is proposed that further experimentation is necessary to specifically define intermediate levels of roughness and lubricant to understand the extent of the dependence of wall shear stress on these two parameters. Figure 28 demonstrates how intermediate data levels would enable better understanding of the nature (linear or decay) and limitations that lubricant addition and surface roughness have on wall shear.

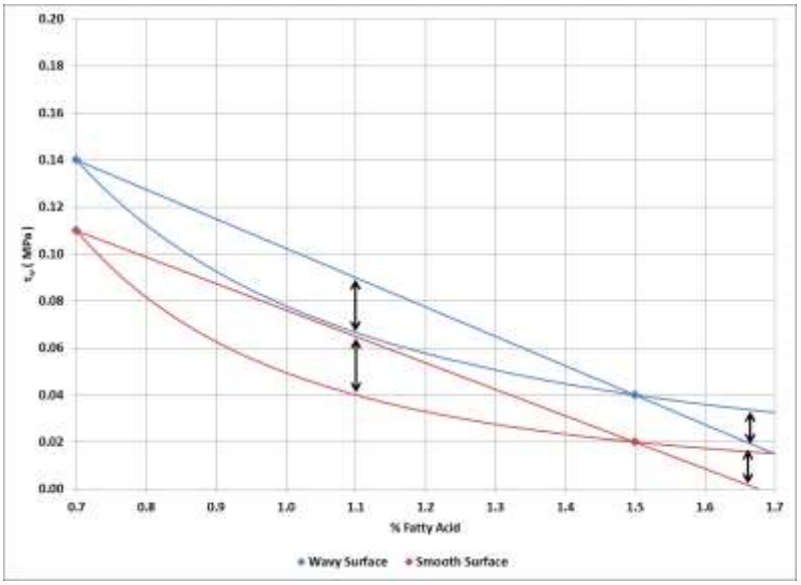

Figure 28. Graph of wall shear stress versus fatty acid percent demonstrating two potential wall shear behaviors due to surface roughness at an extrusion velocity of 25.4 $mm \cdot s^{-1}$.

To create a wider range of surface roughness, capillary dies will be prepared using the correlation of thicknesses to TiCN grain sizes as shown previously in Figure 16 and Figure 17. The lubrication layer presumably changes the lubrication layer thickness for particles to ride on before coming in contact with the die wall. It is hypothesized that as the die wall varies from smooth to rough, the lubricant required to separate batch particles from the die wall increases. Conversely, as the wall gets smoother there is an limit to which lubricant produces appreciable change, thus implying fatty acid levels above this point are not adding to the wall lubrication effect and is thus wasted. Through further experimentation a defined roughness range at intermediate lubricant levels a model can be developed to determine optimal roughness to lubricant ratios for a given surface or process. Figure 29 demonstrates the hypothesized interaction which would be revealed through widely varying surface roughness and lubrication level. This data is important because a power law trend would show that for each surface roughness a point exists beyond which wall shear behavior does not change significantly.

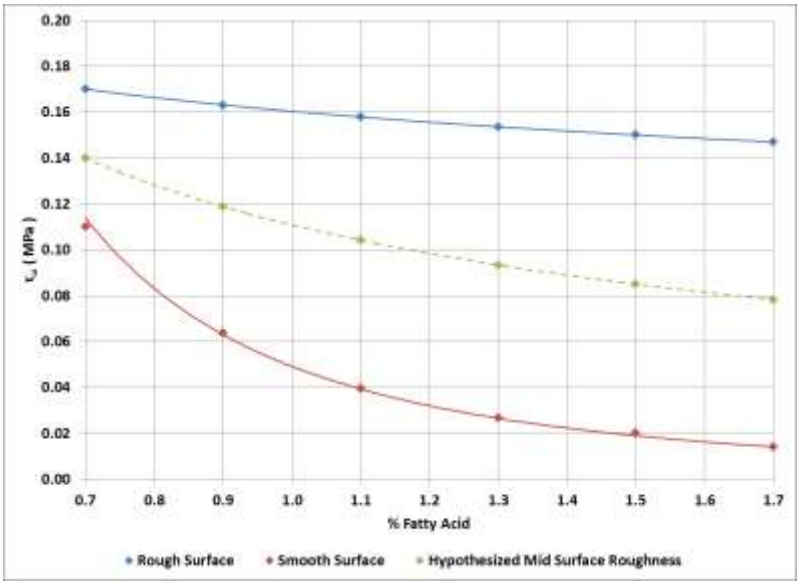

Figure 29. Expected result for testing intermediate surface roughness varying fatty acid level at an extrusion velocity of 25.4 mm·s^{-1}.

Coupled with multiple extrusion velocities, a range of pressure can be exerted against the wall for each surface roughness and fatty acid level combination. Presumably this compresses the lubrication layer until the expression of lubricant is insufficient resulting in a system which relies on low frictional force to maintain plug flow.

REFERENCES

1. J. Zheng, W. B. Carlson, and J. S. Reed, "Flow Mechanics on Extrusion through a Square-Entry Die," *J. Am. Ceram. Soc.,* **75** [11] 3011-6 (1992).

2. R. Bagley, "Extrusion Method for Forming Thinwalled Honeycomb Structures," Pat. US3790654 1974.

3. J. Benbow and J. Bridgwater, *Paste Flow and Extrusion*. Clarendon Press, Oxford, 25-33, 1993.

4. A. U. Khan, B. J. Briscoe, and P. F. Luckham, "Evaluation of Slip in Capillary Extrusion of Ceramic Pastes," *J. Eur. Ceram. Soc.,* **21** [4] 483-91 (2001).

5. D. R. Dinger, *Rheology for Ceramists,* 2nd ed.*;* pp. 1-21, 99-108, 29-46. Edited by D. R. Dinger. Dinger Ceramic Consulting Services, Lexington, KY, 2012.

6. D. I. Wilson and S. L. Rough, "Exploiting the Curious Characteristics of Dense Solid–Liquid Pastes," *Chem. Eng. Sci.,* **61** [13] 4147-54 (2006).

7. C. K. Schoff and P. Kamarchik, *Rheology and Rheological Measurements*. John Wiley and Sons, Inc., New York, NY, 2000.

8. M. N. Rahaman, *Ceramic Processing and Sintering,* 2nd ed.*;* pp. 230-43. Taylor & Francis, 2003.

9. J. S. Reed, *Principles of Ceramics Processing,* 2nd ed.*;* pp. 277-305. John Wiley and Sons, Inc., New York, NY, 1995.

10. H. Barnes, "The Yield Stress -- a Review or "Panta Rei" -- Everything Flows?," *Journal of Non-Newtonian Fluid Mechanics,* **81** 133-78 (1999).

11. J. J. Benbow, E. W. Oxley, and J. Bridgwater, "The Extrusion Mechanics of Pastes—the Influence of Paste Formulation on Extrusion Parameters," *Chem. Eng. Sci.,* **42** [9] 2151-62 (1987).

12. J. J. Benbow, "The Dependence of Output Rate on Die Shape During Catalyst Extrusion," *Chem. Eng. Sci.,* **26** [9] 1467-73 (1971).

13. R. Nath Das, C. D. Madhusoodana, and K. Okada, "Rheological Studies on Cordierite Honeycomb Extrusion," *J. Eur. Ceram. Soc.,* **22** [16] 2893-900 (2002).

14. Z. Corporation, Metropro Surface Texture Parameters, [Computer Program] Zygo Corporation, Middlefield, CT, 2005.

15. M. Sen and H. S. Shan, "A Review of Electrochemical Macro- to Micro-Hole Drilling Processes," *International Journal of Machine Tools and Manufacture,* **45** [2] 137-52 (2005).

16. W. N. Peters, "Shaped-Tube Electrolytic Machining Process," Pat. US5322599 1994.

17. P. C. Pandey and H. S. Shan, *Modern Machining Processes;* pp. 52-6. Tata McGraw-Hill Publishing Company Limited, New Delhi, 1980.

18. S. Hinduja and M. Kunieda, "Modelling of Ecm and Edm Processes," *CIRP Annals - Manufacturing Technology,* **62** [2] 775-97 (2013).

19. J. Pattavanitch and S. Hinduja, "Machining of Turbulated Cooling Channel Holes in Turbine Blades," *CIRP Annals - Manufacturing Technology,* **61** [1] 199-202 (2012).

20. P.-C. Tsai, W.-J. Chen, J.-H. Chen, and C.-L. Chang, "Deposition and Characterization of Tibcn Films by Cathodic Arc Plasma Evaporation," *Thin Solid Films,* **517** [17] 5044-9 (2009).

21. J. Lin, J. J. Moore, M. Pinkas, D. Zhong, and W. D. Sproul, "Tibcn:Cnx Multilayer Coatings Deposited by Pulsed Closed Field Unbalanced Magnetron Sputtering," *Surf. Coat. Technol.,* **206** [4] 617-22 (2011).

22. H. Holzschuh, "Chemical-Vapor Deposition of Wear Resistant Hard Coatings in the Ti–B–C–N System: Properties and Metal-Cutting Tests," *Int. J. of Refract. Met. Hard Mater.,* **20** [2] 143-9 (2002).

23. L. A. Chow, "6 - Equipment and Manufacturability Issues in Cvd Processes"; pp. 127-78 in *Handbook of Thin Film Deposition (Third Edition).* Edited by K. Seshan. William Andrew Publishing, Oxford, 2012.

APPENDIX

Table V. Summary of Terms

Symbol	Meaning
COF	Coefficient of Friction
D	Die Land Diameter
D_0	Capillary Barrel Diameter
K	Coefficient of Rigidity
L	Die Land (Wall) Length
m	Bulk Velocity Exponent
n	Flow Behavior Index
P	Total Extrusion Pressure
P_e	Die Entry Pressure
P_l	Die Land (Wall) Pressure
Ra	Average Surface Micro-roughness
V	Batch Extrusion Velocity
Wa	Average Surface Micro-waviness
α	Velocity Sensitivity Factor
β	Die Land (Wall) Velocity Factor
$\dot{\gamma}$	Shear Rate
η	Paste Viscosity
μ	Newtonian Viscosity Constant
μ_B	Bingham Viscosity Constant
σ	Bulk Yield Stress
τ_0	Initial (Rest) Stress of Paste
τ_s	Shear Stress
τ_ω	Die Land (Wall) Shear Stress
τy	Paste Yield Stress